Modification of Wilkinson's catalyst with triphenyl phosphite: Synthesis, structure, ^{31}P NMR and DFT study of trans-[RhCl(P(OPh)$_3$)(PPh$_3$)$_2$]

Ioannis Choinopoulos [a], Ioannis Papageorgiou [a], Silverio Coco [b], Emmanuel Simandiras [c], Spyros Koinis [a,*]

[a] Laboratory of Inorganic Chemistry, Faculty of Chemistry, National and Kapodistrian University of Athens, Panepistimiopolis, 15771 Athens, Greece
[b] IU/CINQUIMA, Química Inorgánica, Facultad de Ciencias, Universidad de Valladolid, 47071 Valladolid, Spain
[c] Theoretical and Physical Chemistry Institute, National Hellenic Research Foundation, 48 Vassileos Constantinou Avenue, 11635 Athens, Greece

ABSTRACT

The complex trans-[RhCl(P(OPh)$_3$)(PPh$_3$)$_2$] (**1**) has been prepared and characterized by ^{31}P NMR spectroscopy and single crystal X-ray crystallography. It was found that in the solid state there are two forms of complex **1** in the unit cell forming a cocrystal. DFT theoretical computations have confirmed the existence of the two forms and have provided evidence for the greater stability of **1** compared with Wilkinson's catalyst, [RhCl(PPh$_3$)$_3$] (**2**), in terms of the dissociation energy of the Rh-P(PPh$_3$) bonds. On the basis of the phosphorus chemical shifts, δ(P$_{PPh_3}$), and the results of the theoretical computations, it is suggested that the Rh-P(PPh$_3$) bonding interactions are slightly enhanced in **1** compared with **2**. A distinct difference between complexes **1** and **2**, was found to be the catalytic activity of **1** in the alkylation of allyl acetate with sodium diethylmalonate, while **2** is almost catalytically inefficient.

© 2012 Elsevier Ltd. All rights reserved.

1. Introduction

The importance of [RhCl(PPh$_3$)$_3$], Wilkinson's catalyst, in the advance of organometallic chemistry and catalysis is universally recognized [1]. Wilkinson's catalyst has been shown to be an efficient catalyst not only for the homogeneous hydrogenation of unsaturated substrates but also for a large variety of organic reactions [1b,2]. Furthermore, the start of the development of catalysts for asymmetric hydrogenation was the concept of replacing the triphenylphosphine ligand of Wilkinson's catalyst with a chiral ligand [3].

Trivalent phosphorus ligands are ubiquitous in organometallic chemistry and homogeneous catalysis and their primary role is the fine-tuning of the electron density, and consequently of the reactivity, of the metal center in the course of catalytic reactions [4]. This is accomplished through steric and electronic effects first described in detail by Tolman [5]. Thus in the context of the development of new catalysts it is of major importance the understanding of the nature of the effects by which trivalent phosphorus ligands modulate the reactivity of the metal center.

Phosphites (phosphite esters) are extremely attractive ligands for transition metal catalysts. Their available synthesis allows the modification of electronic and steric properties. Metal complexes of phosphites were generally supposed to be inefficient for hydrogenation catalysts, by reason of the putative high π-acidity of the

phosphite ligands [6]. This was revised as soon as hydridophosphitorhodium(I) clusters and mononuclear complexes were found to be efficient hydrogenation catalysts [6,7].

Phosphite ligands have been used widely for the modification of rhodium catalysts bearing phosphine ligands, usually *in situ*. These modifications can be classified in the following three broad categories.

(i) Complexes of the form [(L-L)Rh(P-OP)]$^+$ (L-L = acac, cod, nbd and P-OP = chiral bidentate phosphine-phosphite ligand, e.g. BINAPHOS), which were introduced by Takaya et al. as modifications of the corresponding complexes with chiral biphosphines and have been used as catalyst precursors for homogeneous hydrogenations and hydroformylations [8].
(ii) The *in situ* modification of Wilkinson's catalyst with phosphites, which resulted in highly efficient catalytic systems for allylic alkylation reactions. These were introduced by Tsuji et al. [9] and their applications were extended by Evans et al. [10].
(iii) Complexes of the form [(L-L)RhP^{a}P^b]$^+$ (L-L = cod, P^a = monodentate phosphine, P^b = monodentate phosphite) which were introduced by Reetz et al. and were used in the context of the Combinatorial Enantioselective Transition Metal Catalysis with S-BINOL derived monodentate P-ligands [11].

Although the effect of the phosphite, in the cases of the *in situ* modifications of Wilkinson's catalyst, has been studied from the point of view of the catalytic performance [10,12], the role of the
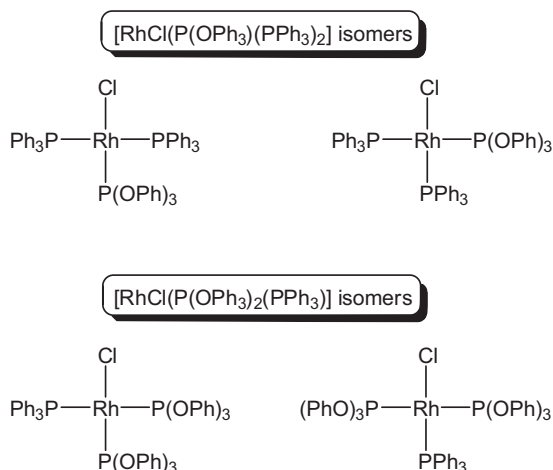
Fig. 1. Possible forms of the triphenyl phosphite modified Wilkinson's catalyst.

phosphite remains unidentified, since nothing is known about the nature of the catalyst precursors and the catalytically active species involved. In most cases the ratio [RhCl(PPh₃)₃]/phosphite used for the modification of Wilkinson's catalyst was in the range 1÷3 to 1÷4. Most probably among the catalyst precursors, the mononuclear Rh(I) complexes with mixed trivalent phosphorus ligands, PPh₃ and phosphite, are an obvious choice. Therefore we began a systematic work towards the synthesis, the characterization and the study of the catalytic activity of Rh(I) complexes with mixed monodentate trivalent phosphorus ligands, phosphines and phosphites, starting with PPh₃ and P(OPh)₃. The only report, to our knowledge, of a Rh(I) complex, in which both PPh₃ and P(OPh)₃ ligands are coordinated is [RhCl(CO)(PPh₃)(P(OPh)₃)] [13].

The possible forms of the modified forms of Wilkinson's catalyst with triphenyl phosphite are, in principle, four; two mono-phosphito and two di-phosphito isomers, Fig. 1.

We, herein, shall describe the synthesis of *trans*-[RhCl(P(OPh)₃)(PPh₃)₂], which is the first structurally characterized modified form of Wilkinson's catalyst with mixed phosphine and phosphite ligands. We shall also discuss the effects induced to the "RhCl(PPh₃)₂" fragment as a result of the substitution of PPh₃ by P(OPh)₃ in terms of structural and ³¹P NMR spectroscopic data, supported by DFT theoretical computations results. Finally we shall present the catalytic performance of *trans*-[RhCl(P(OPh)₃)(PPh₃)₂] in the alkylation of allyl acetate with sodium diethylmalonate.

2. Experimental

2.1. Materials and methods

Starting materials and solvents were purchased from Sigma–Aldrich. [RhCl(PPh₃)₃] [14] and [Rh₂Cl₂(cod)₂] [15] were synthesized according to literature methods. THF and diethyl ether were distilled over Na/Ph₂CO prior to use. The solvents were degassed by bubbling nitrogen for 30 min. All operations were performed under a pure nitrogen atmosphere, using Schlenk and syringe techniques on an inert gas/vacuum manifold. NMR spectra were recorded on a Varian Unity Plus 300 spectrometer. For the ¹H NMR spectra the solvent peak was used as an internal reference and the ³¹P NMR spectra were referenced with an external standard of H₃PO₄ 85%.

2.2. Synthesis of trans-[RhCl(P(OPh)₃)(PPh₃)₂]

2.2.1. 1st method

In a Schlenk tube [RhCl(PPh₃)₃] (0.4626 g, 0.50 mmol) and P(OPh)₃ (0.1551 g, 0.50 mmol) were introduced with CH₃CN

(40 mL). The mixture was stirred and in a few minutes a bright yellow solution resulted. The stirring was continued for 24 h and resulted to the formation of a bright yellow solid. The mixture was condensed to dryness and hexane (20 mL) was added to the solid residue. The mixture was stirred vigorously for 10 min and the light yellow liquid phase was carefully suctioned. Hexane (20 mL) was added and after 10 min of vigorous stirring the yellow solid was collected by filtration and dried in vacuo over P₂O₅. (Yield 0.48 g, 95%). *Anal.* Calcd. for C₅₄H₄₅ClO₃P₃Rh: C, 66.64; H, 4.66; N. Found: C, 66.47; H, 4.38%.

2.2.2. 2nd method

In a Schlenk tube P(OPh)₃ (0.0310 g, 0.10 mmol) and PPh₃ (0.0525 g, 0.20 mmol) were introduced with CH₃CN (10 mL). To the resulting solution [Rh₂Cl₂(cod)₂] (0.0247 g, 0.05 mmol) was added with CH₃CN (10 mL). The reaction mixture was stirred and a bright yellow solution resulted. The stirring was continued for 3 h and then it was condensed to dryness. Hexane (20 mL) was added to the solid residue, the mixture was stirred vigorously for 10 min and the light yellow liquid phase was carefully suctioned. Hexane (20 mL) was added and after 10 min of vigorous stirring the yellow solid was collected by filtration and dried in vacuum over P₂O₅. (Yield 0.024 g, 95%).

2.3. Alkylation of allyl acetate

In a Schlenk tube NaH (0.0348 g, 1.45 mmol) and THF (4 mL) were introduced and diethyl malonate (228 µL, 1.50 mmol) was added dropwise, resulting in the evolution of H₂ gas. This solution was transferred and added slowly by syringe to another Schlenk tube containing *trans*-[RhCl(P(OPh)₃)(PPh₃)₂] (0.0487 g, 0.050 mmol), allyl acetate (54 µL, 0.50 mmol) and THF (4 mL). The reaction mixture was stirred for 19 h at room temperature and an orange solution with a white precipitate resulted. The mixture was condensed until the liquid phase became oily. Diethylether (15 mL) was added and the white solid was filtered and washed with diethylether (10 mL). The filtrate was condensed until an oily liquid remains. The conversion was determined by ¹H NMR spectroscopy.

2.4. Crystallographic analysis

X-ray diffraction measurements were made using a Bruker SMART CCD area-detector diffractometer with Mo Kα radiation (*k* = 0.71073 Å) [16]. Suitable single crystal of the complex was mounted in glass fiber. Intensities were integrated from several series of exposures, each exposure covering 0.3° in ω, the total data set being a hemisphere [17]. Absorption corrections were applied based on multiple and symmetry-equivalent measurements [18]. The structures were solved by direct methods and refined by least squares on weighted *F²* values for all reflections [19]. All non-hydrogen atoms were assigned anisotropic displacement parameters and refined without positional constraints. Hydrogen atoms were taken into account at calculated positions and refined as riding atoms. Complex neutral-atom scattering factors were used [20].

2.5. Computational studies

All calculations were done with the GAUSSIAN 09 suite of programs [21]. The SVP basis is a split-valence plus polarization [22] and the TZVPP is a triple zeta valence plus double polarization including an effective core potential [23,24]. The popular B3LYP functional is due to Becke [25] and Lee et al. [26] and contains empirical data, whereas the fully ab initio PBE functional used is due to Perdew [27]. The TZVPP computations were made faster

using the Density Fitting approximation [28]. The structures were fully optimized and stationary points characterized by second derivative calculations to confirm that they are true minima. The frequencies calculated were used for the estimation of the $v = 0$ level energy differences.
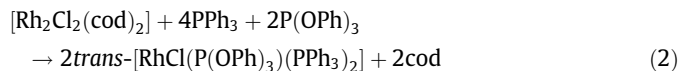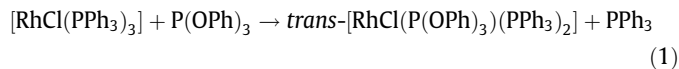
3. Results and discussion

3.1. The system: [RhCl(PPh₃)₃]+n P(OPh)₃

It is impressive that for almost 50 years after the synthesis of Wilkinson's catalyst, the consequent syntheses of a variety of rhodium complexes using Wilkinson's catalyst as starting material and the use of *in situ* modifications of Wilkinson's catalyst with phosphites in homogeneous catalysis, the title complex has not been reported yet. In order to gain some insight into the Rh(I) complexes with mixed PPh₃–P(OPh)₃ ligands we have measured the ^{31}P NMR spectra of [RhCl(PPh₃)₃]+nP(OPh)₃ systems, shown in Fig. 2.

From the spectra it comes out that for $n = 1$, complex **1** is the only rhodium complex present, while the systems for $n = 2$ and 3 are multicomponent systems containing rhodium complexes with mixed PPh₃–P(OPh)₃ ligands. Thus, in order to prepare complex **1**, accurate quantities of the reagents should be used and special precaution should be taken regarding the purity of the easily oxidized triphenyl phosphite.

3.2. Synthesis

The complex *trans*-[RhCl(P(OPh)₃)(PPh₃)₂] (**1**) was prepared quantitatively either by reacting [RhCl(PPh₃)₃] (**2**) with P(OPh)₃ (Eq. (1)) or by reacting [Rh₂Cl₂(cod)₂] with a stoichiometric mixture of PPh₃ and P(OPh)₃, (Eq. (2)):

$$[RhCl(PPh_3)_3] + P(OPh)_3 \rightarrow trans\text{-}[RhCl(P(OPh)_3)(PPh_3)_2] + PPh_3$$

$$(1)$$

$$[Rh_2Cl_2(cod)_2] + 4PPh_3 + 2P(OPh)_3$$
$$\rightarrow 2trans\text{-}[RhCl(P(OPh)_3)(PPh_3)_2] + 2cod \qquad (2)$$

Both reactions can be carried out in acetonitrile, acetone or dichloromethane. Complex **1** can be stored under vacuum in a desiccator, but samples can be weighed in the atmosphere. It can be heated without decomposition (toluene, reflux, 2 h), while Wilkinson's catalyst, under the same conditions is dimerized completely giving [(PPh₃)₂Rh(μ-Cl)₂Rh(PPh₃)₂] [[1b]]. In solution, in the presence of oxygen, it decomposes and a brown solid is formed. It reacts with CO in CH₂Cl₂ solution, yielding labile species even at low temperature as deduced from ^{31}P NMR spectroscopy. Addition of acetone to the solution under CO bubbling results in the precipitation of *trans*-[RhCl(CO)(PPh₃)₂]. The nature of the hydrido species formed in the presence of dihydrogen is under investigation.

The structure of **1** was assigned on the basis of analytical and spectroscopic data. The formation of this species as unique product was demonstrated by measuring the ^{31}P NMR spectra of the reaction mixtures (see Table 1).

3.3. X-ray crystal and molecular structure of 1

Single crystals of **1** suitable for X-ray diffraction measurements, were obtained by slow diffusion of hexane into a solution of the complex in CH₃CN. The crystal examined was found to be a cocrystal of two chemically identical forms of complex **1** in 1÷1 ratio, $Z = 8$. These forms which shall be referred to as **1a** and **1b**, are analogous to the red and orange forms of Wilkinson's catalyst, which crystallize independently depending upon the conditions of synthesis [29]. Selected interatomic distances and bond angles are
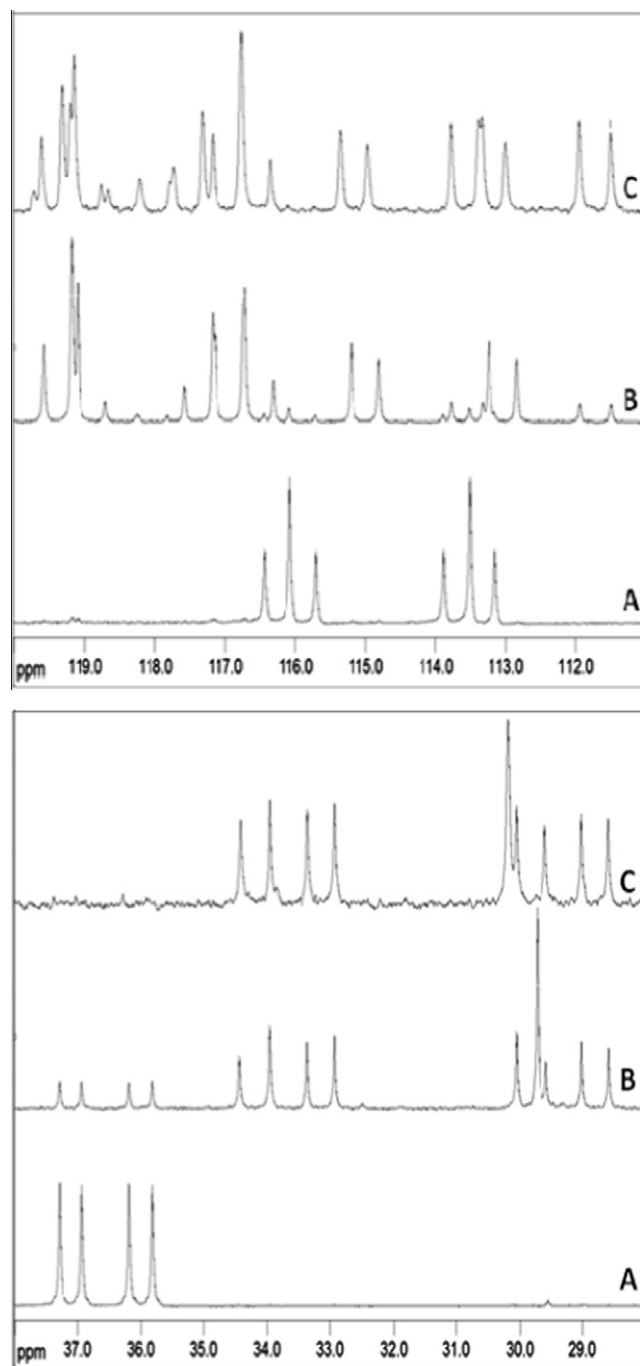

Fig. 2. ^{31}P NMR spectra of [RhCl(PPh₃)₃]+nP(OPh)₃ systems. A: $n = 1$; B: $n = 2$; C: $n = 3$ (upper: P(OPh)₃ region; lower: PPh₃ region).

presented in Table 2. The molecular structures of the two forms of **1**, shown in Figs. 3 and 4, can be described in terms of square planar coordination to a first approximation.

The RhClP₃ fragment for both forms is planar within experimental error. In contrast to this, for both forms of Wilkinson's catalyst there is a distortion toward tetrahedral geometry, which is not due to steric crowding, since, as stated elsewhere, the trans Rh–P bonds are similar to those in the less congested *trans*-[RhCl(CO)(PPh₃)₂], suggesting that steric crowding is not responsible for this distortion, which is also found in [RhCl(PMe₃)₃] [30].

The differences of the Rh–Cl and the Rh–P(PPh₃) bond lengths of the two forms of **1** with the respective bond lengths of Wilkinson's catalyst forms are not significant.

Table 1
Crystal data and structure refinement data for complex **1**.

Complex	1
Formula	$C_{54}H_{45}ClO_3P_3Rh$
M_r	973.17
T (K)	298(2)
λ (Å)	0.71073
Crystal system	orthorhombic
Space group	$Pca2(1)$
a (Å)	25.318(8)
b (Å)	19.138(6)
c (Å)	19.097(6)
α (°)	90
β (°)	90
γ (°)	90
V (Å^3)	9253(5)
Z	8
ρ_{calc} (g m^{-3})	1.397
μ (mm^{-1})	0.574
$F000$	4000
Crystal size (mm)	$0.26 \times 0.24 \times 0.14$
θ_{max} (°)	28.20
No. reflections collected	89378
R_{int}	0.0638
Data	22357
Parameters	1117
R^a [$I > 2\sigma(I)$]	0.0477
$R^a\omega^b$ (all data)	0.0840
R indices (all data)	$R_1 = 0.0840$, $wR_2 = 0.1089$
Residuals (e Å^{-3})	1.248/−0.547

The Rh–P(P(OPh)$_3$) bond lengths are the same within experimental error and significantly shorter compared to the respective Rh–P(PPh$_3$) bonds of Wilkinson's catalyst indicative of a higher bond order, as a result of the σ-donor and π-acceptor nature of P(OPh)$_3$.

The Rh–P(P(OPh)$_3$) bond lengths of the two forms of **1**, 2.1454(12) and 2.1406(12), are among the shortest so far reported: [(cod)Rh(μ-Cl)$_2$Rh(P(OPh)$_3$)$_2$] 2.1378(7), 2.1475(8) Å [31], [(acac)Rh(P(OPh)$_3$)$_2$] 2.147(2), 2.156(2) and 2.142(2), 2.150(2) Å [32] and [(CF$_3$)COCH$_2$C(CH$_3$)O)Rh(P(OPh)$_3$)$_2$] 2.148(4), 2.136(6) and 2.145(6), 2.130(6) Å [33].

A probable explanation of the self-assembling of the two forms of **1** in a cocrystal compared to Wilkinson's catalyst (and the analogous iridium complex [34]) for which the two forms crystallize separately forming different crystals, could be that the two forms of **1** are more closely related both structurally and/or energetically.
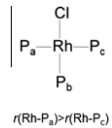
3.4. DFT calculations

The structures of **1** and **2** were fully optimized using Density Functional Theory combined with split-valence (SVP) and larger triple zeta (TZVPP) basis sets using B3LYP and PBE functionals respectively. The data are reported in Table 2.

Firstly it is noted that theoretical computations clearly confirm the existence of two chemically equivalent forms of **1**. These two forms are stable minima of the potential energy surface, which was confirmed by force constant calculations.

The second observation worth noting from Table 2 is that there exists a very good broad agreement between the theoretical and X-ray data, especially for the PBE/TZVPP calculations. Differences of less than 0.005 Å for the Rh–Cl bond lengths are seen, and less than 0.015 Å for the Rh–P lengths, the correct ordering between **1a** and **1b** being well reproduced. The angles are also in good broad agreement; in fact that comparison is between a closely packed cocrystal and a computation for the isolated zero point gas phase structure should be taken into account.

Further, it is seen that our results for **2** are in good broad agreement with the previously reported theoretical results [34]; this is

Table 2
Bond lengths [Å] and bond angles [°] of the two forms of *trans*-[RhCl(P(OPh)$_3$)(PPh$_3$)$_2$] (experimental and *computed* with the B3LYP and PBE functionals) and of Wilkinson's catalyst (experimental [29] and *computed* with the BP86 functional [34]).

$$\begin{array}{c} Cl \\ | \\ P_a\!-\!Rh\!-\!P_c \\ | \\ P_b \end{array}$$

$r(Rh\text{-}P_a) > r(Rh\text{-}P_c)$

Parameter	[RhCl(P(OPh)$_3$)(PPh$_3$)$_2$]		[RhCl(PPh$_3$)$_3$]	
	1a	**1b**	Red	Orange
Rh–Cl (Å)				
X-ray	2.3814(13)	2.3857(13)	2.376(4)	2.404(4)
BP86			2.42	2.42
B3LYP/SVP	2.426	2.431	2.437	2.443
PBE/TZVPP	2.376	2.386		
Rh–P$_a$ *trans* to P$_c$ (Å)				
X-ray	2.3220(12)	2.3146(13)	2.322(4)	2.304(4)
BP86			2.35	2.35
B3LYP/SVP	2.387	2.386	2.392	2.376
PBE/TZVPP	2.335	2.331		
Rh–P$_c$ *trans* to P$_a$ (Å)				
X-ray	2.3236(13)	2.3321(13)	2.334(3)	2.338(4)
BP86			2.37	2.38
B3LYP/SVP	2.401	2.390	2.424	2.434
PBE/TZVPP	2.341	2.340		
Rh–P$_b$ *trans* to Cl (Å)				
X-ray	2.1454(12)	2.1406(12)	2.214(4)	2.225(4)
BP86			2.27	2.27
B3LYP/SVP	2.192	2.189	2.301	2.309
PBE/TZVPP	2.153	2.150		
P$_a$–Rh–Cl (°)	83.64(5)	85.61(5)	86.1(2)	85.3(1)
P$_c$–Rh–Cl (°)	87.41(4)	84.59(5)	85.2(2)	84.5(1)
P$_a$–Rh–P$_b$ (°)	94.89(5)	96.08(4)	97.9(2)	97.7(1)
P$_c$–Rh–P$_b$ (°)	94.06(4)	93.48(4)	100.4(1)	96.4(2)
PBE/TZVPP	85.2, 87.6,	87.4, 84.7,		
	96.1, 98.1	95.1, 95.6		
P$_a$–Rh–P$_c$ (°)	171.03(4)	169.38(4)	152.8(1)	159.1(2)
PBE/TZVPP	155.9	163.7		
Cl–Rh–P$_b$ (°)	172.82(5)	176.41(5)	156.2(1)	166.7(2)
PBE/TZVPP	161.4	165.9		

expected since we are comparing a similar size basis set, for the SVP case, but different functionals. The B3LYP/SVP results, of this work in Table 2 for both molecules clearly show that, overall, the Rh–P(PPh$_3$) bond lengths are shorter for **1** than for **2**. In particular for **2** we find that one of the Rh–P(PPh$_3$) bonds, the Rh–P$_c$ is consistently the longest compared to all other calculated and measured bond lengths for both compounds. The PBE/TZVPP results, which are of much higher quality confirm the consistently shorter Rh–P(PPh$_3$) bonds. Summarizing, the DFT calculations show that **1** exists, even in the gas phase, in two very similar forms which have a common feature, namely that all Rh–P(PPh$_3$) bonds are shorter and hence stronger compared to the corresponding ones in **2**.

The energy differences between the two forms for various levels of theory are given in Table 3. In all cases the energy differences are very small and certainly within the possible range of error for the methods used. However, the consistency observed, and the agreement with a previous study [34], support the findings. It can therefore be concluded that the two forms of **1** are closer in energy compared to the two forms of **2**. This may be the reason for the formation of a cocrystal and not two different crystal allotropes.

A measure of the stability of the compound is the dissociation energy of the two Rh–P(PPh$_3$) bonds. Although it is solvent dependent, a gas phase theoretical calculation can in any case provide a measure of the relative Rh–P(PPh$_3$) bond strengths. This was calculated in Ref. [34] for **2** and found to be 13.9 kcal/mol. For **1**, a phosphine was removed and the two fragments were reoptimized at the PBE/TZVPP level. The dissociation energy was found to be 26.2 kcal/mol (or 25.2 between ν = 0 energy levels), approximately double that of **2**.
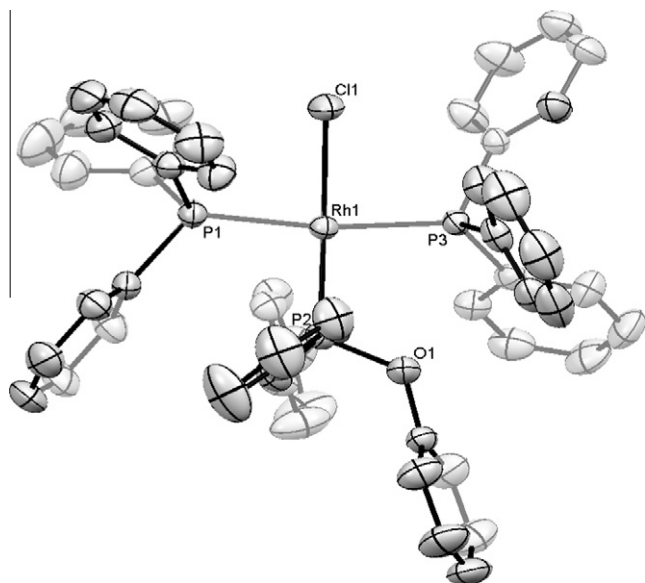
Fig. 3. ORTEP drawing of complex **1a**, projected onto the mean molecular plane RhClP$_3$. Hydrogen atoms have been omitted for clarity. Selected bond lengths and bond angles are reported in Table 1.

Fig. 4. ORTEP drawing of complex **1b**, projected onto the main molecular plane RhClP$_3$. Hydrogen atoms have been omitted for clarity. Selected bond lengths and bond angles are reported in Table 1.
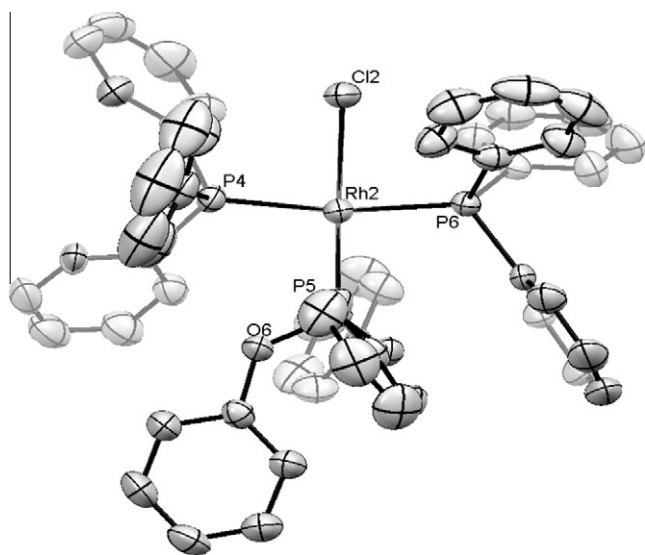
3.5. ^{31}P NMR

The ^{31}P NMR spectral parameters of complex **1** are presented in Table 4. The only signals observed in the spectrum of **1**, are a *dd* (2P, PPh$_3$ region) and a *dt* (1P, P(OPh)$_3$ region), which are assigned to the coordinated phosphorus ligands.

Although the X-ray molecular structures do not provide any significant differentiation for **1** compared with **2** in terms of the Rh–P(PPh$_3$) bond lengths of their common fragments, RhCl(PPh$_3$)$_2$, the ^{31}P NMR spectra provide such a differentiation, namely the spectral parameters of the, *cis* to the chlorine, PPh$_3$. As shown in Table 4, for **1** compared with **2**, the chemical shift, δ(P$_{PPh_3}$), is shifted to higher frequencies (downfield) and the spin–spin coupling constant ^1J(Rh–P$_{PPh_3}$) is reduced.

Table 3
Computed energy differences (in kcal/mol) for the two forms of **1** and **2**.

	1	**2**
B3LYP/SVP		
eq	0.8	1.9
v = 0	1.2	1.7
PBE/TZVPP		
eq	1.0	
v = 0	1.4	

Table 4
^{31}P NMR spectral parameters of the complexes [RhCl(X)(PPh$_3$)$_2$] (X=P(OPh)$_3$, PPh$_3$).

Complex	δ(P)/ppm PPh$_3$	δ(P)/ppm P(OPh)$_3$	^1J(Rh–P)/Hz Rh–PPh$_3$	^1J(Rh–P)/Hz Rh–P(OPh)$_3$	^2J(P–P)/Hz
1	36.57	114.81	134.4	310.8	44.6
2	31.07*dd*		143.7		36.9
	48.05*dt*		192.1		36.9

The variation of the ^{31}P NMR parameters of the, *cis* to the chlorine, PPh$_3$ can be used to probe the *cis*-electronic effect induced as a result of the substitution of the, *trans* to the chlorine, PPh$_3$ (class II phosphorus ligand, σ-donor) of [RhCl(PPh$_3$)$_3$] by P(OPh)$_3$ (class III phosphorus ligand, σ-donor and π-acceptor) [35].

These are in accordance with the ^{31}P NMR spectrum of *trans*-[RhCl(Ppyrl$_3$)(PPh$_3$)$_2$] (Ppyrl$_3$: *N*-pyrrolylphosphine; class III phosphorus ligand), which shows two distinct sets of phosphorus resonances: a *dd* due to the pair of mutually *trans* PPh$_3$ ligands (δ (P) 34.3 ppm, ^1J(Rh–P) 133 Hz, ^2J(P–P) 42 Hz) and a *dt* assignable to the unique P(pyrl)$_3$ ligand (δ (P) 101.1 ppm, ^1J(Rh–P) 278 Hz, ^2J(P–P) 42 Hz) [36]. The variation of the ^{31}P NMR parameters, of *trans*-[RhCl(Ppyrl$_3$)(PPh$_3$)$_2$] compared with **2**, are in the same direction with those found for **1**. Thus it is seen that upon substitution of the, *trans* to the chlorine, PPh$_3$, of Wilkinson's catalyst by σ-donors/π-acceptors phosphorus ligands the chemical shift, δ (P$_{PPh_3}$), tends to be shifted to higher frequencies.

3.6. Comments on the variation of the Rh–P(PPh$_3$) bonding

An interpretation of the observed variation of δ (P$_{PPh3}$), for **1** compared to **2**, in terms of respective variation in Rh–P(PPh$_3$) bonding interactions can thus be given taking into account the following:

(a) In the case of Wilkinson's catalyst the formation of the dimer [(PPh$_3$)$_2$Rh(μ-Cl)$_2$Rh(PPh$_3$)$_2$] has been correlated with the dissociation of triphenylphosphine according to the following reactions [1b,37]:
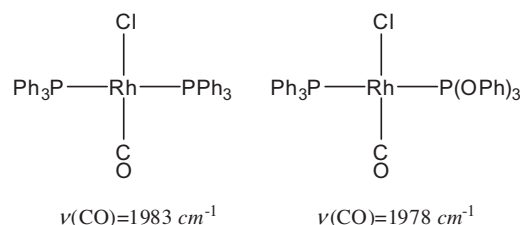
$$[RhCl(PPh_3)_3] \rightleftharpoons [RhCl(PPh_3)_2] + PPh_3 \qquad (3)$$

$$2[RhCl(PPh_3)_2] \rightleftharpoons [(PPh_3)_2Rh(\mu\text{-}Cl)_2Rh(PPh_3)_2] \qquad (4)$$
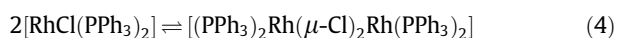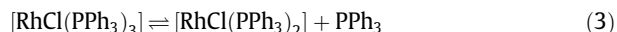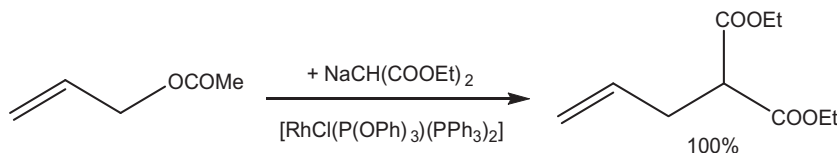

Fig. 5. P(OPh)$_3$ *cis*-effect in mixed PPh$_3$–P(OPh)$_3$ rhodium carbonyl species.

Scheme 1. Alkylation of allyl acetate catalyzed by 1.

As mentioned above DFT computations provide evidence of enhancement of the Rh–P(PPh$_3$) bonds for **1** compared with **2**, which are based on the calculated bond dissociation energies and bond lengths. Thus the aforementioned stability of **1** with respect to dimerization could be attributed to an enhancement of Rh–P(PPh$_3$) bonding interactions of **1** relative to **2**.

(b) A *cis*-effect induced by P(OPh)$_3$ can be recognized by comparing of the carbonyl vibrational frequencies of the complexes *trans*-[RhCl(CO)(PPh$_3$)$_2$] and [RhCl(CO)(P(OPh)$_3$)(PPh$_3$)] [13], Fig. 5. The slight decrease of ν(CO) could be attributed, to a crude approximation, to the fine-tuning of the Rh–C bond order towards enhancement [38].

(c) The interpretation of the ^{31}P NMR coordination chemical shifts, $\Delta\delta$(P), equal to the difference between the chemical shift upon coordination, δ(P)$_c$, and the chemical shift of the free phosphorus ligand, δ(P)$_f$, in terms of the σ-donor and π-acceptor abilities of these ligands has been pioneered by Alyea et al. [39]. According to a comprehensive discussion they have proposed that: (i) predominantly electronic, rather than steric, factors are active in determining δ (P) and both the sign and the magnitude of the coordination chemical shift $\Delta\delta$(P) in terms of σ- and π-electronic effects and (ii) both σ(M $\leftarrow$ P) and π(M $\rightarrow$ P) components should bring ^{31}P chemical shift to high frequency. These proposals were based on the theoretical treatment of the chemical shift of the free phosphorus ligands according to which the ^{31}P NMR chemical shifts are thought to arise primarily from variations in the paramagnetic contribution from electrons in valence orbitals [40]. Ziegler et al., have conducted an elaborate theoretical study (DFT-GLIAO) of the ^{31}P NMR chemical shifts for complexes of the type [M(CO)$_5$PR$_3$] (M=Cr, Mo; R=H, CH$_3$, C$_6$H$_5$, F and Cl) which has confirmed the domination of the paramagnetic shielding term in determining the phosphorus chemical shift [41].

It can thus be suggested that in complex **1** the withdrawal of electron density, from rhodium to P(OPh)$_3$ through π-bonding interaction (backbonding) together with the diminished σ electron donor capacity of P(OPh)$_3$ as compared with PPh$_3$, is compensated by the enhancement of the Rh–P(PPh$_3$), bonding interactions. This variation is not reflected explicitly in the solid state Rh–P(PPh$_3$) bond lengths and should be considered as a fine tuning, towards enhancement.

3.7. Alkylation of allyl acetate

trans-[RhCl(P(OPh)$_3$)(PPh$_3$)$_2$] was found to catalyze the alkylation of allyl acetate with sodium diethylmalonate in THF. See Scheme. 1.

Tsuji et al. have reported that although [RhCl(PPh$_3$)$_3$] showed almost no activity in the allylic alkylation, highly efficient catalytic systems have resulted by the addition of P^{n}Bu$_3$ or P(OEt)$_3$ and, Evans et al. have reported that efficient "modified" catalysts were formed *in situ*, by using mixtures of [RhCl(PPh$_3$)$_3$] and phosphites (P(OPh)$_3$, P(OMe)$_3$) in a 1÷3 molar ratio [9,10]. Our finding showed

that *trans*-[RhCl(P(OPh)$_3$)(PPh$_3$)$_2$] is the first well defined Rh complex with mixed trivalent phosphorus ligands that catalyzes effectively an allylic alkylation reaction.

4. Conclusions

In summary, the synthesis of the modified form of Wilkinson's catalyst with triphenyl phosphite, *trans*-[RhCl(P(OPh)$_3$)(PPh$_3$)$_2$], was accomplished using as starting materials either [RhCl(PPh$_3$)$_3$] or [Rh$_2$Cl$_2$(cod)$_2$]. The X-ray crystal structure showed the presence of two forms of **1** in the unit cell, forming a cocrystal. Based on experimental, spectroscopic and computational data it is suggested that the result of the substitution of the *trans*, to the chlorine, PPh$_3$ of Wilkinson's catalyst by P(OPh)$_3$ is the fine enhancement of the Rh–P(PPh$_3$) bonding interactions in **1** compared with **2**, in agreement with the superior thermal stability of **1** in solution compared with Wilkinson's catalyst.

This low cost modification of Wilkinson's catalyst resulted in an efficient catalyst precursor for the alkylation of allyl acetate with sodium diethylmalonate, while [RhCl(PPh$_3$)$_3$] is almost catalytically inactive.

Appendix A. Supplementary data

CCDC 699645 contains the supplementary crystallographic data for **1**. These data can be obtained free of charge via http://www.ccdc.cam.ac.uk/conts/retrieving.html, or from the Cambridge Crystallographic Data Centre, 12 Union Road, Cambridge CB2 1EZ, UK; fax: +44 1223-336-033; or e-mail: deposit@ccdc.cam.ac.uk.

References

[1] (a) M.A. Bennett, P.A. Longstaff, Chem. Ind. (London) (1965) 846;
(b) J.A. Osborn, F.H. Jardine, J.F. Young, G. Wilkinson, J. Chem. Soc. A (1966) 1711.
[2] For a review, see: F.H. Jardine, Prog. Inorg. Chem. 28 (1981) 63.
[3] W.S. Knowles (Nobel Lecture), Adv. Synth. Catal. 345 (2003) 3.
[4] (a) R.P. Hughes, in: G. Wilkinson, F.G.A. Stone, E.W. Abel (Eds.), Comprehensive Organometallic Chemistry, Pergamon Press, Oxford, UK, 1982. Chapter 35;
(b) P.R. Sharp, in: G. Wilkinson, F.G.A. Stone, E.W. Abel (Eds.), Comprehensive Organometallic Chemistry II, vol. 8, Pergamon Press, Oxford, UK, 1995. Chapter 2;
(c) L.H. Pignolet (Ed.), Homogeneous Catalysis with Metal Phosphine Complexes, Plenum, New York, 1983.
[5] C.A. Tolman, Chem. Rev. 77 (1977) 313.
[6] H.K.A.C. Coolen, R.J.M. Nolte, P.W.N.M. van Leeuwen, J. Organomet. Chem. 496 (1995) 159.
[7] A.J. Sivak, E.L. Muetterties, J. Am. Chem. Soc. 101 (1979) 4878.
[8] (a) N. Sakai, S. Mano, K. Nozaki, H. Takaya, J. Am. Chem. Soc. 115 (1993) 7033;
(b) H. Fernández-Pérez, S.M.A. Donald, I.J. Munslow, J. Benet- Buchholz, F. Maseras, A. Vidal-Ferran, Chem. Eur. J. 16 (2010) 6495 (and references therein).

 [9] J. Tsuji, I. Minami, I. Shimizu, Tetrahedron Lett. 25 (1984) 5157.
[10] (a) P.A. Evans, J.D. Nelson, Tetrahedron Lett. 39 (1998) 1725;
     (b) P.A. Evans, J.D. Nelson, J. Am. Chem. Soc. 120 (1998) 5581.
[11] (a) M.T. Reetz, G. Mehler, Tetrahedron Lett. 44 (2003) 4593;
     (b) M.T. Reetz, G. Mehler, A. Meiswinkel, Tetrahedron: Asymmetry 15 (2004) 2165;
     (c) M.T. Reetz, Angew. Chem., Int. Ed. 47 (2008) 2556.
[12] U. Kazmaier, D. Stolz, Angew. Chem., Int. Ed. 45 (2006) 3072.
[13] D.M. Barlex, M.J. Hacker, R.D.W. Kemmit, J. Organomet. Chem. 43 (1972) 425.
[14] J.A. Osborn, G. Wilkinson, Inorg. Synth. 28 (1990) 77.
[15] G. Giordano, R.H. Crabtree, Inorg. Synth. 28 (1990) 88.
[16] SMART V5.051 Diffractometer Control Software, Bruker Analytical X-ray Instruments Inc., Madison, WI, 1998.
[17] SAINT V6.02 Integration Software, Bruker Analytical X-ray Instruments Inc., Madison, WI, 1999.
[18] G.M. Sheldrick, SADABS: A Program for Absorption Correction with the Siemens SMART System, University of Göttingen, Göttingen, Germany, 1996.
[19] SHELXTL Program System Version 5.1, Bruker Analytical X-ray Instruments Inc., Madison, WI, 1998.
[20] International Tables for Crystallography, vol. C, Kluwer, Dordrecht, 1992.
[21] G.W.T.M.J. Frisch, H.B. Schlegel, G.E. Scuseria, M.A. Robb, J.R. Cheeseman, G. Scalmani, V. Barone, B. Mennucci, G.A. Petersson, H. Nakatsuji, M. Caricato, X. Li, H.P. Hratchian, A.F. Izmaylov, J. Bloino, G. Zheng, J.L. Sonnenberg, M. Hada, M. Ehara, K. Toyota, R. Fukuda, J. Hasegawa, M. Ishida, T. Nakajima, Y. Honda, O. Kitao, H. Nakai, T. Vreven, J.A. Montgomery Jr., J.E. Peralta, F. Ogliaro, M. Bearpark, J.J. Heyd, E. Brothers, K.N. Kudin, V.N. Staroverov, R. Kobayashi, J. Normand, K. Raghavachari, A. Rendell, J.C. Burant, S.S. Iyengar, J. Tomasi, M. Cossi, N. Rega, J.M. Millam, M. Klene, J.E. Knox, J.B. Cross, V. Bakken, C. Adamo, J. Jaramillo, R. Gomperts, R.E. Stratmann, O. Yazyev, A.J. Austin, R. Cammi, C. Pomelli, J.W. Ochterski, R.L. Martin, K. Morokuma, V.G. Zakrzewski, G.A. Voth, P. Salvador, J.J. Dannenberg, S. Dapprich, A.D. Daniels, Ö. Farkas, J.B. Foresman, J.V. Ortiz, J. Cioslowski, D.J. Fox, Gaussian 09, Revision A.1, Gaussian Inc., Wallingford CT, 1996.
[22] R. Ahlrichs, K. May, Phys. Chem. Chem. Phys. 2 (2000) 943.
[23] F. Weigend, R. Ahlrichs, Phys. Chem. Chem. Phys. 7 (2005) 3297.
[24] D. Andrae, U. Haussermann, M. Dolg, H. Stoll, H. Preuss, Theor. Chim. Acta 77 (1990) 123.
[25] A.D. Becke, Phys. Rev. A 38 (1988) 3098.
[26] C.T. Lee, W.T. Yang, R.G. Parr, Phys. Rev. B 37 (1988) 785.
[27] (a) J.P. Perdew, K. Burke, M. Ernzerhof, Phys. Rev. Lett. 78 (1997) 1396;
     (b) J.P. Perdew, K. Burke, M. Ernzerhof, Phys. Rev. Lett. 77 (1996) 3865.
[28] B.I. Dunlap, J. Mol. Struct. THEOCHEM 529 (2000) 37.
[29] M.J. Bennett, P.B. Donaldson, Inorg. Chem. 16 (1977) 655.
[30] S.A. Cotton, The Chemistry of Precious Metals, Blackie Academic & Professional, London, 1997. pp. 90.
[31] J. Coetzer, G. Gaffner, Acta Crystallogr., Sect B: Struct. Crystallogr. Cryst. Chem. 26 (1970) 985.
[32] G.L. Lamprecht, J.G. Leipoldt, G.J. Van Zyl, Inorg. Chim. Acta 96 (1985) L31.
[33] G.J. Van Zyl, G.L. Lamprecht, J.G. Leipoldt, Inorg. Chim. Acta 102 (1985) L1.
[34] J. Goodman, V.V. Grushin, R.B. Larichev, S.A. Macgregor, W.J. Marshall, D.C. Roe, J. Am. Chem. Soc. 132 (2010) 12013.
[35] M.N. Golovin, M.M. Rahman, J.E. Belmonte, W.P. Giering, Organometallics 4 (1985) 1981.
[36] C.R. Landis, S. Feldgus, J. Uddin, C.E. Wozniak, K.G. Moloy, Organometallics 19 (2000) 4878.
[37] D.A. Wink, P.C. Ford, J. Am. Chem. Soc. 109 (1987) 436.
[38] F.A. Cotton, G. Wilkinson, Advanced Inorganic Chemistry, fifth ed., Wiley, New York, 1988. pp. 58.
[39] E.C. Alyea, S. Song, Inorg. Chem. 34 (1995) 3864.
[40] J.H. Letcher, J.R. Van Wazer, J. Chem. Phys. 44 (1966) 815.
[41] Y. Ruiz-Morales, T. Ziegler, J. Phys. Chem. A 102 (1998) 3970.